Available online at www.sciencedirect.com
ScienceDirect
Advances in Space Research 38 (2006) 1750–1754
ADVANCES IN SPACE RESEARCH (a COSPAR publication)
www.elsevier.com/locate/asr

Plasma convection in the Earth's magnetosphere and ionosphere during substorms

M. Förster [a,*], V.M. Mishin [b], P. Stauning [c], J. Watermann [c], T.I. Saifudinova [b], A.D. Bazarzhapov [b]

[a] Max-Planck-Institut für extraterrestrische Physik, P.O. Box 1312, D-85741 Garching, Germany
[b] Institute of Solar-Terrestrial Physics, Russian Academy of Sciences, P.O. Box 4026, Irkutsk 664033, Russia
[c] Danish Meteorological Institute, Lyngbyvej 100, DK-2100 Copenhagen, Denmark

Received 16 August 2004; received in revised form 30 November 2005; accepted 26 March 2006

Abstract

The empirical field-aligned current (FAC) and plasma convection model on which this paper is based describes the four phases of a typical substorm. 2D maps of the ionospheric electric potential (U) are shown here for the first time for each of these phases. The principal result is the identification of medium-scale ionospheric convection vortices, which are observed in addition to the well-known two large-scale DP2 convection cells. We conclude that these convection vortices are the analogue to the heterogeneities that were found earlier in the spatial distribution of the FAC density. They had been taken into account there in the framework of the conceptual model of magnetospheric generators. This model is extended in the present paper such that it also describes the above-mentioned medium-scale convection vortices.
© 2006 COSPAR. Published by Elsevier Ltd. All rights reserved.

Keywords: Convection; Field-aligned currents; Substorms; M–I coupling

1. Introduction

Several different concepts exist in substorm theory, but essentially only two alternative basic scenarios, which are related to the current disruption (CD) model of Lui (1996) and the near-Earth neutral line (NENL) model of Baker et al. (1996), respectively. The synthesis of these two basic concepts leads to the scenario of a substorm with two successive active phases and/or two types of substorm onsets, one of those corresponding to the CD model and the other to the NENL concept. Based on their Magnetogram Inversion Technique (MIT2), Mishin et al. (2003a,b, 2005) elaborated an empirical model of the 2-D spatial distribution of field-aligned current (FAC) densities. This model describes a substorm scenario of four successive phases: growth phase, the two different active phases mentioned above, and the recovery phase. The major progress of this model consists in the inclusion of the observed medium-scale heterogeneities in the spatial FAC density distribution. They are more or less regular substructures within the well-known FAC regions of Iijima and Potemra (1976, 1978), and they appear as individual distinctive features of each substorm phase.

During the last decade, global optical observations of the auroral arc resulted in much progress in understanding of the dynamics of polar cap boundaries and its relation to substorm expansion (Brittnacher et al., 1999; Newell et al., 2001; Mende et al., 2003). Substorm-related changes in the polar cap convection were also reported from observations using digital ionosondes and the SuperDARN radar network (cf., e.g., Jayachandran et al., 2003).

Note that spatial FAC density distributions for high AE values are also described in the new statistical model of

* Corresponding author. Present address: GeoForschungsZentrum Potsdam, Telegrafenberg, D-14473 Potsdam, Germany. Tel.: +49 331 2881776; fax: +49 331 2881235.
E-mail address: mfo@gfz-potsdam.de (M. Förster).

0273-1177/$30 © 2006 COSPAR. Published by Elsevier Ltd. All rights reserved.
doi:10.1016/j.asr.2006.03.029

Weimer (2001), but without discrimination of substorm phases. Kamide et al. (1996) described FAC distributions for three substorm phases (i.e., with a single active phase), by use of their KRM method. On the whole, the above FAC heterogeneities were obviously overlooked in the past, although they do not contradict some well-known observational material, e.g., those cited in the paper of Weimer (2001). The conceptual model of the magnetospheric generators (Mishin et al., 2003a,b, 2005) accounts for these novel facts on a qualitative level. In this connection, the objective of the present paper is to test the model with observed substorm events and to present the inclusion of the convection aspect into the model with heterogeneities. Four substorms were studied by the authors. Due to the limited space, only one typical example will be described in this paper. A publication with details of the study is in preparation.

MIT2 is based on two Eqs. (1 and 2) which follow from Ohm's law. They are solved numerically in spherical coordinates in order to calculate the ionospheric electric potential U and the FAC density j_z and its temporal development. These equations are the following:

$$\mathrm{curl}(\Sigma \cdot \nabla U) = \Delta J \tag{1}$$

$$\mathrm{div}(\Sigma \cdot \nabla U) = j_z \tag{2}$$

Here, $J(\theta, t)$ is the current function, obtained from ground-based magnetometer measurements as a function of magnetic co-latitude θ and magnetic local time t, $\Sigma(\theta, t)$ is the given tensor of ionosphere conductance, and curl, div, ∇, and Δ are all 2D-operators. We used a spatially homogeneous ionosphere conductance model for the calculation of FAC density j_z and a more realistic non-uniform empirical model of conductance for the calculation of the ionospheric convection (potential U).

The reason for this is the following. If we assume for simplicity $\Sigma(\theta, t) = \mathrm{const}$ we obtain

$$U = J/\Sigma_{\mathrm{H}} \tag{3}$$

$$j_z = (\Sigma_{\mathrm{P}}/\Sigma_{\mathrm{H}})\Delta J \tag{4}$$

where the subscripts H and P stand for Hall and Pedersen conductance, respectively. It is known that the current function $J(\theta, t)$ is represented by the series of Legendre polynomials $P_n^m(\cos\theta)$, the coefficients of which are multiplied by $(2n+1)/(n+1)$, while ΔJ is represented by the same series with coefficients multiplied by $n(2n+1)$, which is quadratic in n. Thus in the spatial distributions of J and U on the one hand and j_z on the other dominate lower and higher order spherical harmonics, respectively, while the relative calculation errors of the coefficients are growing substantially with increasing n. According to our experience in using the MIT2 technique for the analysis of substorm events in many previous studies, the calculated data of j_z need spatial smoothing. This smoothing can be provided without any loss of necessary information about j_z by using $\Sigma(\theta, t) = \mathrm{const}$. For the calculation of U, in contrary, no smoothing is needed (cf., e.g., Mishin, 1990; Kamide and Baumjohann, 1993; and references therein).

2. Ionospheric convection patterns

Among the substorms considered in our analysis is an event from November 22, 1995, 1340–1730 UT which will be described in this paper. Fig. 1 shows the solar wind parameters from the Wind spacecraft, the open tail magnetic flux Ψ (from MIT2), and the AE indices. We determined the lag time of the solar wind parameters to the magnetopause with the standard advection technique, i.e., dividing the x-separation distance measured in GSE coordinates between the Wind spacecraft and the magnetopause position at 10 R_E by the solar wind plasma bulk velocity. The open tail magnetic flux Ψ is calculated from each individual polar cap area pattern obtained independently from each other with the MIT2 technique. These parameters were then used for the timing of the substorms, with the four substorm phases being indicated with roman numerals (Mishin, 1990; Mishin et al., 2001).

Fig. 2 shows the spatial distribution of both the FAC density (top panels) and the ionospheric electric potential U (bottom panels). Let us start with Fig. 2 (top) containing the data of FAC density. Three well-known regions of Iijima and Potemra (1976, 1978) are clearly seen in this figure with their boundaries marked by solid red lines. The main

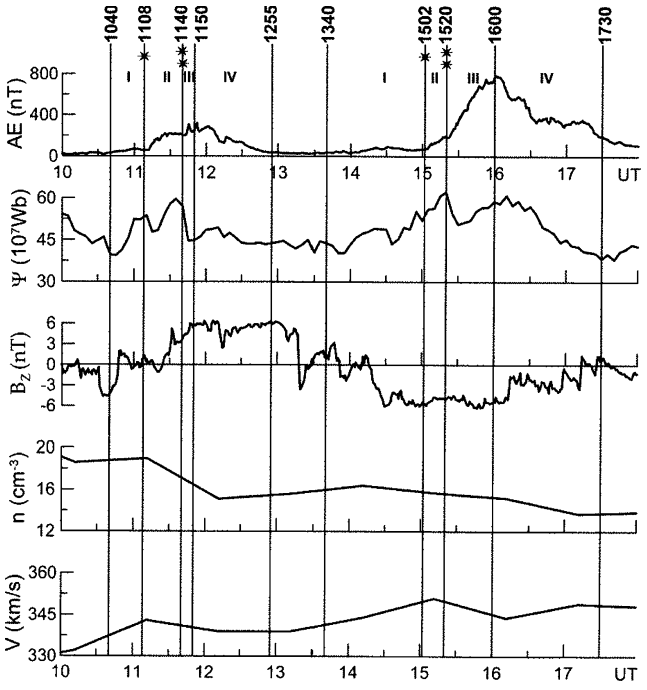

Fig. 1. Solar wind and other parameters of the two substorm events of this study from November 22, 1995 versus UT. From top to bottom: the AE index, open tail magnetic flux Ψ, IMF B_z component, solar wind density and velocity. The four substorm phases are indicated by the roman numerals I–IV for both intervals. The one and two star symbols (*) indicate the commencement of the first and second active phase, respectively.

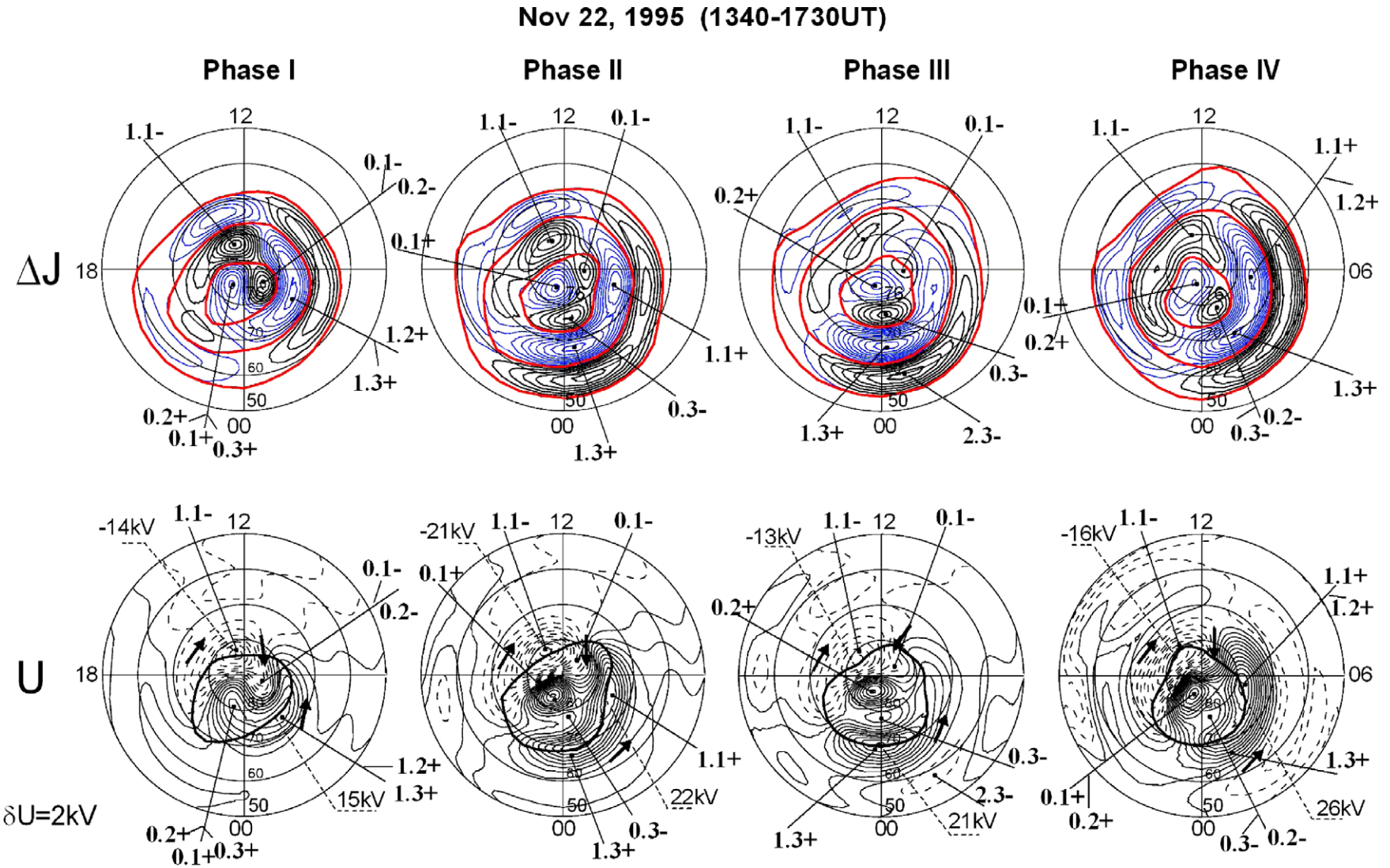

Fig. 2. Case study of November 22, 1995, 13:40–17:30 UT. The top row shows isocontour plots of the FAC density in the ionosphere. The black (blue) thin lines represent upward (downward) currents; the solid red lines are the boundaries of the Iijima-and-Potemra FAC regions (Iijima and Potemra, 1976, 1978). Geomagnetic latitudes correspond to the concentric circles at 50°, 60°, 70°, and 76°. The bottom row shows the isocontours of the ionospheric electric potential at the same time moments. Solid (dashed) lines indicate positive (negative) potential values while the solid black arrows help to identify the direction of the plasma flow.

new element of the FAC model are three types of heterogeneities within each Iijima-and-Potemra region labeled by the symbols "RM.N" (or in short only "M.N"). Here, R stands for "Region", M signifies the Iijima-and-Potemra number of FAC Region with $M = 0$, 1, or 2, and N is the number of the type of heterogeneity ($N = 1$, 2, or 3) for the different zones. The three types of heterogeneities denotes three pairs of FACs: one near the noon meridian ($N = 1$), one near the dawn–dusk meridian ($N = 2$), and the third one near midnight ($N = 3$), all with FACs flowing in opposite directions in the morning and evening sectors.

For instance, the pair of downward (to the ionosphere) and upward FACs in Region 1 near the noon meridian at latitudes of $\Phi \sim 70$–$80°$ is named R1.1+ and R1.1−. The data of Fig. 2 are in good accordance with those of the statistical model of Mishin et al. (2001, 2003a,b).

Now consider Fig. 2 (bottom). Isolines of U in this figure represent convection stream lines. The potential pattern are obtained with a spatially in-homogenous ionosphere conductance model, which is adapted for each instance individually according to Mishin et al. (1986).

Note that inflowing (outflowing) FACs should create convection vortices in the ionosphere with anti-clockwise (clockwise) rotation in the northern (southern) hemisphere (e.g., Cowley et al., 2000). The FAC patterns in Fig. 2 (top) should therefore on a qualitative level correspond to the ionospheric convection patterns. To demonstrate this for our event, the M.N type numbering of the convection cells is applied to the bottom row of Fig. 2 in accordance with the FAC presentations.

We will compare here, as one typical example, the data of the top and bottom rows in Fig. 2 for phase 1. One can see in the top row that the downward and upward FACs of Regions 1 and 0 form two spirals, one inside of the other, with both spirals in the morning and evening sectors twisted clockwise. The bottom row shows also two spirals, one inside the other, twisted clockwise in the morning and evening sectors. It is obvious that the directions of FACs and the plasma convection follow the expected above noted electrodynamic relation. This applies to the two spirals at large, but also individually to each pair of cells with the same M.N number. According to the model, cell 1.1− in the top row (upward FAC) should correspond to a clockwise convection vortex in the bottom row. This is indeed confirmed by the observations. The same holds for the two cells numbered 0.1− and 0.2− in top and bottom rows. The cells 1.2+ and 1.3+ in top row (downward FAC) corresponds to anticlockwise convection vortices in the bottom row as expected. Comparing the pairs 0.2+, 0.1+, and 0.3+ in both rows leads to similar results.

To recapitulate, we have examined a typical example of a substorm and shown that convection patterns contain the same substructures as the corresponding FAC regions with their density maxima M.N. For each of the four substorm phases of the event considered we identified convection cells or traces of them, which correspond to the FAC cells with the same symbol M.N as expected from the spatial FAC density distribution model by Mishin et al. (2003a). This has not been reported before.

Not all individual cells identified in the FAC density distribution can also be detected in the convection systems. Furtheron, the centers of convection vortices in Fig. 2 (bottom) are slightly shifted relative to those of FAC density. These differences refer to an only qualitative, not quantitative, accordance between heterogeneities in the spatial FAC density and electric potential distributions. They might be due to the spatial non-uniformity of ionospheric conductance.

Further details from Fig. 2 to be noted include the following. The convection intensity is highly variable. It increases, in particular, during the substorm onset within the first and second active phases in correspondence with the AE index increase, and remains at about the same level during phase IV. The distribution of the electric potential U deviates from symmetry about the noon–midnight meridian; a clockwise rotation of the whole convection pattern is observed. This is probably related to the positive IMF-B_y component (up to about 6 nT), which is observed during the most part of this event (not shown). A tendency of increased rotation with increasing activity is observed. This tendency is particularly obvious in Region 1 during phase III.

3. Conclusions

(i) During the substorm events considered here, medium-scale ionospheric convection vortices are observed additionally to the two well-known large-scale DP2 convection cells. They are generated by three types of irregular substructures of FACs in each of the three regions of the Iijima and Potemra pattern.
(ii) The intensity of the convection vortices as shown in Fig. 2 increases during the first and second active phases in direct correlation with the AE index increase.
(iii) The potential distribution differs from symmetry about the noon–midnight meridian: a clockwise rotation of the whole pattern is observed.
(iv) A tendency of increased clockwise rotation with increasing activity is also observed. This is most obvious in phase III and in Region 1.
(v) The clockwise rotation mentioned above under item 3 is not only a westward expansion, but also a poleward shifting of the current jets and of the convection streams. The increased rotation during the transition from the first active phase to the second is therefore interpreted as the transition from the CD regime in the lower latitude closed parts of the auroral oval to the NENL regime.

Acknowledgements

This paper results from the common project between the German and Russian science organisations DFG-RFFI

(436 RUS 113/671) and RFBR-DFG (02-05-04002), and it is partly supported by the Grants INTAS 01-0142, RFBR 02-05-64159. The authors from ISTP are grateful to the staff of the ISTP MIT group for the technical help. The authors thank for providing the geomagnetic data: Drs. O. Troshichev (AARI), S. Solovyev (IKFIA), A. Zaitsev (IZMIRAN), A. Vinnitsky (IKIR), E. Kharin (WDC-B), T. Iyemori (WDC-C2), K. Yumoto (210° MM), the Canadian Space Agency (CANOPUS), A. Viljanen (Image), DMI (Greenland chain), J. L. Posch (MACCS), the Geological Survey of Canada, T. Hansen, K. Hayashi, R. Nakamura, S. Nozawa, G. Rostoker, and K. Sh-iokawa. Solar wind and IMF data are courtesy of the Wind-MFI and Wind-SWE teams (R. Lepping, K. Ogilvie, J. Steinberg, and A. Lasarus).

References

Baker, D.N., Pulkkinen, T.I., Angelopoulos, V., Baumjohann, W., McPherron, R.L. Neutral line model of substorms: past results and present view. J. Geophys. Res. 101 (A6), 12,975–13,010, 1996.

Brittnacher, M., Fillingim, M., Parks, G., Germany, G., Spann, J. Polar cap area and boundary motion during substorms. J. Geophys. Res. 104 (A6), 12,251–12,262, 1999.

Cowley, S.W.H. Magnetosphere–ionosphere interactions: a tutorial review, in: Ohtani, S.-I., Fujii, R., Hesse, M., Lysak, R.L. (Eds.), Magnetospheric Current Systems. Vol. 118 of Geophysical Monograph. American Geophysical Union, pp. 91–106, 2000.

Iijima, T., Potemra, T.A. The amplitude distribution of the field-aligned currents at northern high latitudes observed by TRIAD. J. Geophys. Res. 81, 2165–2174, 1976.

Iijima, T., Potemra, T.A. Large-scale characteristics of field-aligned currents associated with substorms. J. Geophys. Res. 83, 599–615, 1978.

Jayachandran, P.T., MacDougall, J.W., Donovan, E.F., Ruohoniemi, J.M., Liou, K., Moor-croft, D.R., St.-Maurice, J.-P. Substorm associated changes in the high-latitude ionospheric convection. Geophys. Res. Lett. 30 (20), 2003.

Kamide, Y., Baumjohann, W. Magnetosphere–Ionosphere Coupling. Springer Verlag, Berlin-Heidelberg, 1993.

Kamide, Y., Sun, W., Akasofu, S.-I. The average ionospheric electrodynamics for the different substorm phases. J. Geophys. Res. 101 (Al), 99–110, 1996.

Lui, A.T.Y. Current disruption in the Earth's magnetosphere: observations and models. J. Geophys. Res. 101 (A6), 13,067–13,088, 1996.

Mende, S.B., Carlson, C.W., Frey, H.U., Peticolas, L.M., Stgaard, N. FAST and IMAGE-FUV observations of a substorm onset. J. Geophys. Res. 108 (A9), 2003.

Mishin, V.M. The magnetogram inversion technique and some applications. Space Sci. Rev. 53, 83–163, 1990.

Mishin, V.M., Forster, M., Bazarzhapov, A.D., Saifudinova, T.I., Karavaev, Y.A., Stauning, P., Watermann, J., Golovkov, V., Solovyev, S. Space weather parameters, computed on the basis of the Magnetogram Inversion Technique. Chin. J. Space Sci. 25 (5), 436–446, 2005.

Mishin, V.M., Lunyushkin, S.B., Shirapov, D.S., Baumjohann, W. A new method for generating instantaneous ionospheric conductivity models using ground-based magnetic data. Planet. Space Sci. 34, 713–722, 1986.

Mishin, V. M., Mishin, V.V., Shirapov, D.S., Golovkov, V.P., Förster, M. Electric field and field-aligned currents of Region 1 and Region 0 generators during the substorm load phase, in: Proceedings of the International Symposium in memory of Yuri Galperin on 'Auroral Phenomena and Solar-Terrestrial Relations'. IKI, Moscow, 4–7 February 2003, pp. 105–112, 2003a.

Mishin, V. M., Shirapov, D. S., Golovkov, V. P., Förster, M. Field-aligned currents of Region 0 as electric shield of the polar cap ionosphere, in: Proceedings of the International Symposium in memory of Yuri Galperin on 'Auroral Phenomena and Solar-Terrestrial Relations'. IKI, Moscow, 4–7 February 2003, pp. 250–256, 2003b.

Mishin, V.M., Saifudinova, T.I., Bazarzhapov, A.D., Russell, C.T., Baumjohann, W., Nakamura, R., Kubyshkina, M. Two distinct substorm onsets. J. Geophys. Res. 106 (A7), 13,105–13,118, 2001.

Newell, P.T., Liou, K., Sotirelis, T., Meng, C-I. Polar Ultraviolet Imager observations of global auroral power as a function of polar cap size and magnetotail stretching. J. Geophys. Res. 106 (A4), 5895–5905, 2001.

Weimer, D.R. An improved model of ionospheric electric potentials including substorm perturbations and application to the Geospace Environment Modeling November 24, 1996, event. J. Geophys. Res. 106, 407–416, 2001.